

# Endocytic delivery of intramolecularly quenched substrates and inhibitors to the intracellular yeast Kex2 protease<sup>1</sup>

M. Kerstin HENKEL<sup>\*2</sup>, Gregory POTT<sup>\*</sup>, Andreas W. HENKEL<sup>\*2</sup>, Luiz JULIANO<sup>†</sup>, Chih-Min KAM<sup>‡</sup>, James C. POWERS<sup>‡</sup> and Alex FRANZUSOFF<sup>\*3</sup>

<sup>\*</sup>Department of Cellular and Structural Biology and CU Cancer Center, University of Colorado Health Sciences Center, Box B111, 4200 East Ninth Avenue, Denver, CO 80262, U.S.A., <sup>†</sup>Department of Biophysics, Escola Paulista de Medicina, Sao Paulo 04044-020, Brazil, and <sup>‡</sup>School of Chemistry and Biochemistry, Georgia Institute of Technology, Atlanta, GA 30332-0400, U.S.A.

Kex2 in the yeast *Saccharomyces cerevisiae* is a transmembrane, Ca<sup>2+</sup>-dependent serine protease of the subtilisin-like pro-protein convertase (SPC) family with specificity for cleavage after paired basic amino acids. At steady state, Kex2 is predominantly localized in late Golgi compartments and initiates the proteolytic maturation of pro-protein precursors that transit the distal secretory pathway. However, Kex2 localization is not static, and its itinerary apparently involves transiting out of the late Golgi and cycling back from post-Golgi endosomal compartments during its lifetime. We tested whether the endocytic pathway could deliver small molecules to Kex2 from the extracellular medium. Here we report that intramolecularly quenched fluoro-

genic substrates taken up into intact yeast revealed fluorescence due to specific cleavage by Kex2 protease in endosomal compartments. Furthermore, the endocytic delivery of protease inhibitors interfered with Kex2 activity for precursor protein processing. These observations reveal that the endocytic pathway does intersect with the cycling itinerary of active Kex2 protease. This strategy of endocytic drug delivery has implications for modulating SPC protease activity needed for hormone, toxin and viral glycoprotein precursor processing in human cells.

**Key words:** endocytosis, precursor protein processing, *Saccharomyces cerevisiae*, secretory pathway.

## INTRODUCTION

Cellular proteins are post-translationally modified during their transit through compartments of the secretory pathway. The serine proteases required for the maturation of precursor proteins in the eukaryotic secretory pathway constitute the subtilisin-like pro-protein convertases or SPC proteases (for reviews, see [1–3]). Unlike the bacterial subtilisins, the Ca<sup>2+</sup>-dependent SPC proteases cleave after the paired basic amino acids Lys-Arg or Arg-Arg. In yeast, the maturation of the  $\alpha$ -factor pheromone precursor to bioactive mating peptides is initiated by the SPC protease Kex2 [4,5]. The discovery and characterization of the yeast Kex2 was instrumental in the identification of mammalian SPC homologues (i.e. furin, PC1/PC3, PC2, PC4, PACE4, PC5/6 and PC7/PC8/LPC) which function in the secretory pathway for the maturation of precursor proteins, such as polypeptide hormones, cytokines, cell surface receptors, toxins and the glycoproteins of enveloped viruses, such as HIV and influenza (see refs. cited in [3]).

The transmembrane Kex2 protease 'resides' in late Golgi compartments at steady state, as detected by indirect immunofluorescence [6,7] and by subcellular fractionation [8–10]. The late Golgi compartments perform the sorting of soluble vacuolar and secretory proteins for delivery to their different destinations [11–16]. However, based on studies with Kex2 harbouring mutations in sorting signals within the cytoplasmic tail, or with

Kex2 localization in clathrin (*chc*) and vacuolar sorting (*vps*) mutants, it was concluded that Kex2 cycles to and is retrieved from the pre-vacuolar compartment, a post-Golgi, endosomal organelle (for review, see [17]). The pre-vacuolar compartment/endosome serves as the intersection for proteins (i) endocytosed from the plasma membrane, (ii) destined for transport to the vacuole, and (iii) for membrane proteins to be recycled back to the Golgi [17,18].

Given that Kex2 cycles through endosomes as part of its trafficking itinerary, the protease is therefore predicted to be accessible to small molecules delivered to endosomes from the extracellular medium by endocytosis. Endocytosis in yeast cells includes fluid-phase, membrane and receptor-mediated internalization from the plasma membrane via endocytic vesicles to endosomal compartment(s) with subsequent traffic to the vacuole [19–21]. To test the hypothesis that the endocytic pathway intersects with the trafficking itinerary of active Kex2 protease, yeast was incubated with endocytic markers, intramolecularly quenched (IQ) fluorogenic peptides and protease inhibitors.

## MATERIALS AND METHODS

### Yeast strains and culturing

The *Saccharomyces cerevisiae* strains used in this study are: BJ926 (MAT $\alpha$ /MAT $\alpha$  TRP1/*trp1*, his1/HIS1, pep4-3/*pep4-3*,

Abbreviations used: Abz, aminobenzyl; CPY, carboxypeptidase Y; HA, haemagglutinin; IQ, intramolecularly quenched; MCA, peptidyl-methyl coumarin 7-amide; SPC, subtilisin-like pro-protein convertase; ssKex2, secreted soluble Kex2.

<sup>1</sup> This work is dedicated to the memory of Victor Franzusoff, who spent four decades working to build bridges of trust between the U. S. and the Soviet Union through the Voice of America.

<sup>2</sup> Present address: Abteilung Molekulare Zellforschung, Max-Planck-Institut für Medizinische Forschung, D-69120 Heidelberg, Germany.

<sup>3</sup> To whom correspondence should be addressed (e-mail Alex.Franzusoff@UCHSC.Edu).

*prb-1122/prb-1122, prc1-407/prc1-407*, from Yeast Genetic Stock Center, Berkeley, CA, U.S.A.); AFY490 or pG5-kex2 $\Delta$ C3/CBO23 (MATa *ura3, leu2, trp1, ade2, pep4::HIS3, prb1::HISG, prc1A::HISG, cir<sup>0</sup>*), provided by R. Fuller and described in [22]; AFY427 (Matx, *ade2, his3-11,-15, leu2-3,-112, trp1-1, ura3-1, can1-100, kex2::HIS3*), described in [23], was mated with BFY101-11c (MATa *his3, leu2-3,-112, kex2::URA3-1* (provided by R. Fuller) to generate diploid AFY697; AFY913 was created by transforming pOKH {the plasmid for expressing OKH (provided by G. Waters [24]) into AFY648 (Matx *ade2-101, ura3-52, his3 $\Delta$ 200, trp1 $\Delta$ , sec14-1<sup>ts</sup>*, provided by V. Bankaitis). OKH stands for Och1-Kex2-HA, which is an engineered fusion protein consisting of the mannosyltransferase, Och1p, followed by a Kex2 cleavage-recognition sequence from the alpha-factor pro-protein, followed by a haemagglutinin (HA) epitope tag sequence for recognition by the 12C3A5 anti-HA monoclonal antibody. YPD [1% yeast extract (Difco), 2% peptone (Difco), 2% glucose] or YNB-glucose [0.67% yeast nitrogen base without amino acids (Difco), 2% glucose] plus amino acid supplements media were used for culturing yeast strains, where 2% agar (Difco) was included for solid media. One  $D_{600}$  unit of yeast is  $\sim 10^7$  cells.

### Chemical synthesis of protease substrates and inhibitors

IQ fluorogenic peptides were synthesized as described [25]. The amino acids for the synthesized substrates were derived from the recognition sequence at the cleavage junction in HIV-1 glycoprotein 160 (gp160): V-V-Q-R-E-K-R-A-V-G (referred to as IQ-gp160); or the substrate with a single amino acid substitution at the cleavage site: V-V-Q-R-E-K-A-A-V-G (referred to as IQ-gp160R>A). The synthesis of the amidine-containing peptidyl-phosphonates has been described previously [26]. Two inhibitors were used in this study: (i) (Z-blocked) carbobenzoxy-Lys-(4-amidinophenylglycine) diphenylamino (4-amidinophenyl) methane phosphonate, which is structurally similar to the paired basic (K-R) Kex2 recognition sequence and will be referred to as the K-R inhibitor; and (ii) which is similar to the K-R inhibitor, but the critical Lys is substituted by Ser, and will be referred to as the S-R derivative.

### Enzyme assays

Secreted soluble Kex2 (ssKex2) was purified as described previously [22,23]. Assays of ssKex2 activity to cleave pre-pro  $\alpha$ -factor *in vitro* under the influence of various inhibitors were performed, and protein concentration was estimated as described [23,27]. The reaction conditions used for IQ fluorogenic substrates were similar to those described for peptidyl-methyl coumarin 7-amide (MCA) substrates [22]. The rate of formation of the free aminobenzyl group (Abz) was determined with a Farrand Manual Spectrofluorimeter S/N 213, equipped with a xenon lamp (200–1400 nm) and a magnetic xenon arc stabilizer ( $\lambda_{\text{excitation}}$  320 nm;  $\lambda_{\text{emission}}$  420 nm). The concentration of the substrates IQ-gp160 and IQ-gp160R>A and the amount of released Abz were normalized for standard solutions of Abz-Phe-Arg-*p*-nitroanilide after complete alkaline and tryptic hydrolysis [28]. Kinetic data for Kex2 were determined by assaying 130 units of ssKex2 with 4.4–30  $\mu$ M IQ-gp160 in 5 min at 37 °C. One unit of ssKex2 activity was defined as 1 pmol of Abz released per min. For kinetics of Kex2 inhibition by the amidine-containing peptidyl phosphonates, 130 units ssKex2 were pre-incubated at 37 °C with 0.1–1 mM inhibitor for 5–30 min. The activity of the enzyme was afterwards determined by the release of Abz fluorescence from 4  $\mu$ M IQ-gp160 in 5 min at 37 °C. The

kinetic parameters  $K_m$  and  $V_{\text{max}}$  for Kex2 with the IQ-gp160 substrate were determined from Lineweaver–Burk plots of the assay data.

### Endocytosis of intramolecularly quenched fluorogenic substrates and vital dyes

Yeast cells were grown overnight at 25 °C to a  $D_{600}$  of 0.5. For each experiment cells with a  $D_{600}$  of 1 were harvested and resuspended to a density of 10  $D_{600}$ /ml in YPD medium. When needed, preincubations were performed with addition of 0.5 mM inhibitor from a 50 mM stock solution in DMSO for 30 min at 25 °C, whereas temperature-sensitive *sec* mutants were preshifted to 37 °C for 20 min. For staining, cells were incubated at 25 °C or 37 °C for the indicated times with 0.6 mM IQ peptides from a 60 mM stock solution in DMSO or with 16  $\mu$ M FM4-64 dye from a 1.6 mM stock solution in water. FM4-64 was provided by Dr. W. J. Betz (University of Colorado Health Sciences Center). The cells were collected at 13000 *g* for 10 s, then resuspended to a density of 25  $D_{600}$  in fresh YPD medium for microscopy.

### Fluorescence microscopy and image processing

Yeast cells were immobilized on microscope slides as described previously [29]. Images were viewed with a Leitz Laborlux epifluorescence microscope equipped with a 100 W Hg lamp, a 20% neutral density transmission filter and a Zeiss 100 $\times$  oil immersion objective. Bandpass filters (Omega Optical, Inc.) in slide holders were used for excitation and emission. Excitation for the IQ fluorogenic substrates and FM4-64 imaging was obtained with 10 nm bandpass filters, 430–440 nm and 541–551 nm respectively. Emitted light from the fluorogenic substrates was sent through a 100 nm bandpass filter (500–600 nm) and a Leitz H3 dichroic mirror; for FM4-64, a 100 nm bandpass filter (600–700 nm) and a Leitz N2 dichroic mirror were used. Images were taken with a Photometrics Star I chilled charge-coupled-device camera (3 s exposure time, gain: 4), stored and analysed on a Silicon Graphics Personal Iris UNIX workstation (software for image processing purchased from G. W. Hannaway & Associates). For comparison of the absolute staining brightness of cells by the IQ fluorogenic substrates, the images were processed only by identical global linear intensity stretching. In order to obtain the best possible resolution and contrast from FM4-64, weakly stained images were enhanced by maximal stretching between the lowest and the brightest pixels in the picture (for details see [30]).

### Pulse–chase radiolabelling and immunoprecipitation

AFY913 yeast were grown overnight at 25 °C in YNB-glucose with the appropriate supplements, then washed and resuspended to 2  $D_{600}$ /ml in the same medium without or with the peptidyl phosphonate derivatives. Cells were shaken with the inhibitors for 90 min, then [<sup>35</sup>S]TranS-Label was added at 50  $\mu$ Ci per  $D_{600}$  unit of yeast for 10 min at 25 °C and an aliquot was diluted 2-fold with 20 mM sodium azide on ice. The remaining cells were incubated in the presence of 0.4% L-methionine, 0.3% L-cysteine in 50 mM ammonium sulphate for a 20 min chase period, then diluted 2-fold with 20 mM sodium azide on ice. Cells were harvested by centrifugation and lysed with glass beads and urea/SDS lysis buffer, as described previously [23]. Immunoprecipitations were performed on 1.5  $D_{600}$  units of lysate for OKH precipitation using 1  $\mu$ l of 12C3A5 mouse monoclonal antibody to the HA epitope (Boehringer Mannheim), or 0.5  $D_{600}$  units of lysate for carboxypeptidase Y (CPY) precipitation using

2  $\mu$ l of anti-CPY rabbit serum [23]. Immunoprecipitates were washed and resolved on 8% SDS gels for fluorography as previously described [23]. Quantification was performed by PhosphorImager analysis (Molecular Dynamics).

## RESULTS

### Kex2 cleaves fluorogenic IQ substrates in a sequence-specific manner

IQ fluorogenic peptides are proven substrates for the SPC proteases Kex2, furin, PC1 and PC2 [31–34]. The principle of the IQ substrates is that the fluorogenic group Abz emits light upon separation from the quenching ethylenediamine dinitro phenyl

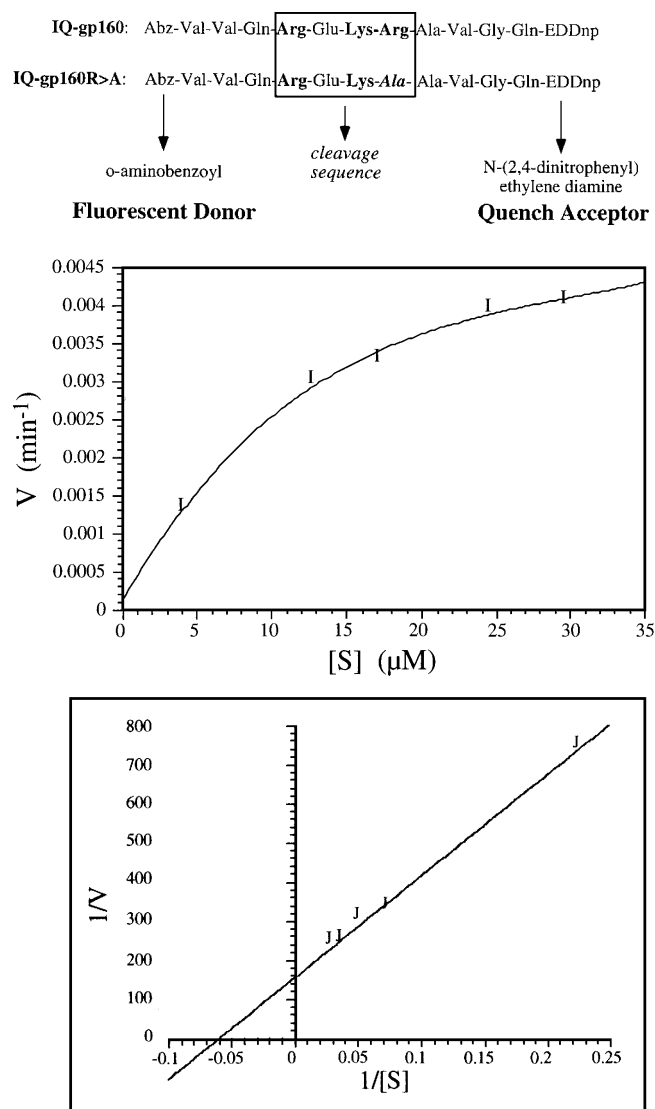


**Figure 1** Kinetic parameters of Kex2 processing of IQ-gp160 substrate

Top: sequences and organization of the IQ-gp160 and IQ-gp160R>A substrates. The boxed area highlights the four residues N-terminal to the SPC protease-cleavage junction. Bottom: two representations of Kex2 kinetic data are shown: Michaelis–Menten graph of velocity  $V$  versus  $[S]$  and the Lineweaver–Burk plot ( $1/V$  versus  $1/[S]$ ) of the same assay data, using 130 units of ssKex2 per assay point, varying the IQ-gp160 substrate concentration and measuring the production of fluorescence from substrate cleavage at 25 °C. The apparent  $K_m$  was calculated to be 15.46  $\mu$ M,  $V_{max}$  was 0.376  $s^{-1}$ .

(EDDnp) group (Figure 1A). We designed two undeca-peptides, IQ-gp160 and the mutant IQ-gp160R>A, for studies with Kex2 protease. The peptide in IQ-gp160 contains the cleavage-recognition sequence for the SPC-dependent maturation of HIV-1 gp160, which is processed by Kex2 in yeast [23]. The R>A peptide has a substitution of alanine for the essential arginine required by Kex2 for substrate recognition [35]. To evaluate the IQ peptides as protease substrates, kinetic measurements were performed with purified ssKex2 at 4.4–30  $\mu$ M peptide. Though kinetic measurements with natural Kex2 substrates have not been reported, the  $K_m$  of the IQ-gp160 substrate is 15.5  $\mu$ M (Figure 1B). This value is similar to that previously reported (2.2–19  $\mu$ M) for IQ peptides and MCA substrates with different protease-recognition sequences [22,33]. The  $V_{max}$  for the IQ-gp160 was substantially less than for previously reported model substrates, suggesting that the gp160 recognition sequence was not efficiently cleaved by the yeast Kex2 protease. This is consistent with the observation that gp160 expressed in yeast was processed with fidelity, yet inefficiently, *in vivo* [23]. The IQ-gp160R>A peptide, however, was not cleaved by ssKex2, though alkaline treatment or incubation with trypsin yielded the fluorescence expected from hydrolysis of the R>A derivative (results not shown). Hence, IQ-gp160, but not IQ-gp160R>A, served as a moderately effective Kex2 substrate *in vitro*, suggesting that these IQ substrates would be useful for evaluating Kex2 activity *in vivo*.

### *In vivo* uptake and cleavage of the IQ substrates in yeast cells

The endocytic pathway in yeast includes uptake from the plasma membrane through intermediate compartments *en route* to the vacuole. The lipophilic styryl dye, FM4-64, behaves as a membrane tracer of the yeast endocytic pathway in a temperature-, time- and energy-dependent manner [29]. In these experiments, diploid BJ926 yeast incubated with 16  $\mu$ M FM4-64 was examined by fluorescence microscopy. In 5–20 min at 25 °C the internalized dye revealed multiple small fluorescent structures (Figures 2A and 2E). At 30 min, both punctate and vacuolar membrane staining were visible (Figure 2E). After 45 min, the staining was almost exclusively localized to membranes of the yeast vacuole (Figure 2I). The distribution of the yeast vacuoles for co-localization with the FM4-64 dye staining was also monitored by Nomarski (differential interference contrast) microscopy (results not shown), as previously described [29].

The time course of endocytosis with intact yeast cells was repeated with the soluble IQ-gp160 and IQ-gp160R>A fluorogenic peptides. Earlier attempts to visualize endocytic structures with commercially available MCA-coupled peptide substrates for Kex2 were unsuccessful because the fluorescent marker liberated from the peptide was freely diffusible and lipophilic, causing the signal to dissipate rapidly (results not shown). In contrast, the fluorescent Abz group from the IQ substrates remains associated with charged residues of the cleaved peptide sequence and therefore does not diffuse rapidly from the site of cleavage. Incubation of BJ926 yeast with medium containing 0.6 mM IQ-gp160 at 25 °C began to reveal intracellular punctate staining at 5 min (Figure 2B), similar to the pattern seen at early time points with the FM4-64 dye. This pattern intensified over 30 min incubation (Figure 2F), then faded after 60 min.

Changes in the progression of FM4-64 dye distribution and IQ-gp160 processing-dependent fluorescence were examined in temperature-sensitive *sec* mutants known to block membrane traffic in yeast endocytic and secretory pathways. In wild-type yeast at 37 °C, FM4-64 dye marked small intracellular compartments after 10 min incubation, then highlighted vacuolar mem-

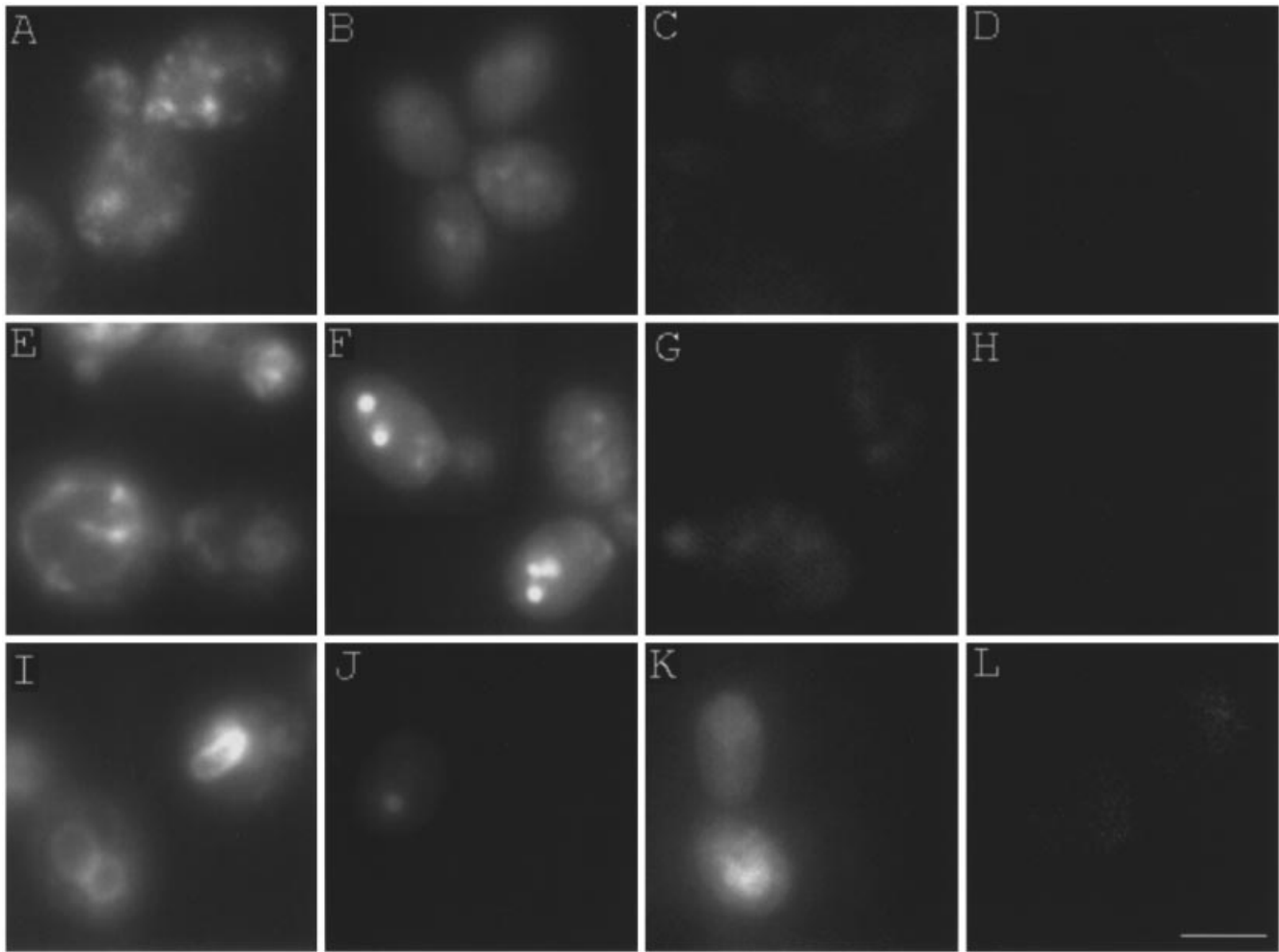


**Figure 2** Kex2 processing activity within the endocytic pathway of yeast cells

Kex2<sup>+</sup> BJ926 diploid yeast (panels A–C, E–G, I–K) and Kex2-deficient AFY697 yeast (panels D, H, L) were incubated either with 16  $\mu$ M FM4-64 (A, E, I), 0.6 mM IQ-gp160 (B, F, J and D, H, L) or with 0.6 mM IQ-gp160R>A (C, G, K). Cells were viewed by fluorescence microscopy after 5 (A–D), 30 (E–H) or 60 (I–L) min incubation. The results shown are representative of four experiments. Scale bar = 5  $\mu$ m.

branes after 45 min incubation (Figure 3, top panels, under A). IQ-gp160 peptide fluorescence was visible in the small intracellular compartments at 10 min incubation (Figure 3, top panel, under B). At 45 min incubation, the IQ-gp160-dependent fluorescence still highlighted the small intracellular compartments and was very distinct from the pattern of FM4-64 fluorescence seen in the vacuoles at the same time point. These results reiterate that IQ-gp160 cleavage takes place in endosomal compartments *en route* to, yet not in, the vacuoles of wild-type cells.

A functional endocytic pathway was essential to the normal progression of either FM4-64 trafficking or IQ-gp160 processing. No intracellular signal was observed when FM4-64 dye or the IQ-gp160 substrate were incubated with *sec18* mutant yeast at the restrictive temperature (Figure 3, middle panels, under A and B). Endocytosis is blocked in *sec18* mutants due to the accumulation of endocytic vesicles unable to access early or late endosomes [21]. A different phenotype was revealed by incubating FM4-64 dye and IQ-gp160 peptide with *sec7* mutants at the restrictive temperature. Both fluorescent compounds accumulated in small intracellular structures, which did not change over the time course of incubation (Figure 3, bottom panels, under A

and B). The *sec7* mutant caused endocytic traffic to the vacuole from endosomes to be disrupted. This is consistent with the previously reported defects in  $\alpha$ -factor internalization in *sec7* mutants, which prevented traffic from the endosomes [36]. In contrast, no defects in either FM4-64 traffic or IQ-gp160 processing were observed in *sec13* mutants shifted to the restrictive temperature (results not shown), indicating that functioning of the secretory pathway is not necessarily essential for endocytic traffic.

The requirement for Kex2 activity in the specific cleavage of the IQ-gp160 substrate was shown in several ways. First, the IQ-gp160 peptide did not fluoresce in the endosomes of AFY490 yeast lacking the Kex2 gene product (Figures 2D, 2H and 2L). In a second approach, the fate of the IQ-gp160R>A peptide, which is not cleaved by Kex2 *in vitro*, was examined. When incubated with intact yeast, fluorescence from the IQ-gp160R>A peptide appeared much later (30 min) than from the IQ-gp160 substrate (Figures 2C, 2G and 2K). The fluorescent signal from IQ-gp160R>A highlighted the vacuole in a similar manner to that seen with the FM4-64 dye at similar incubation time points (Figure 2I). Therefore the Kex2-dependent fluorescence from

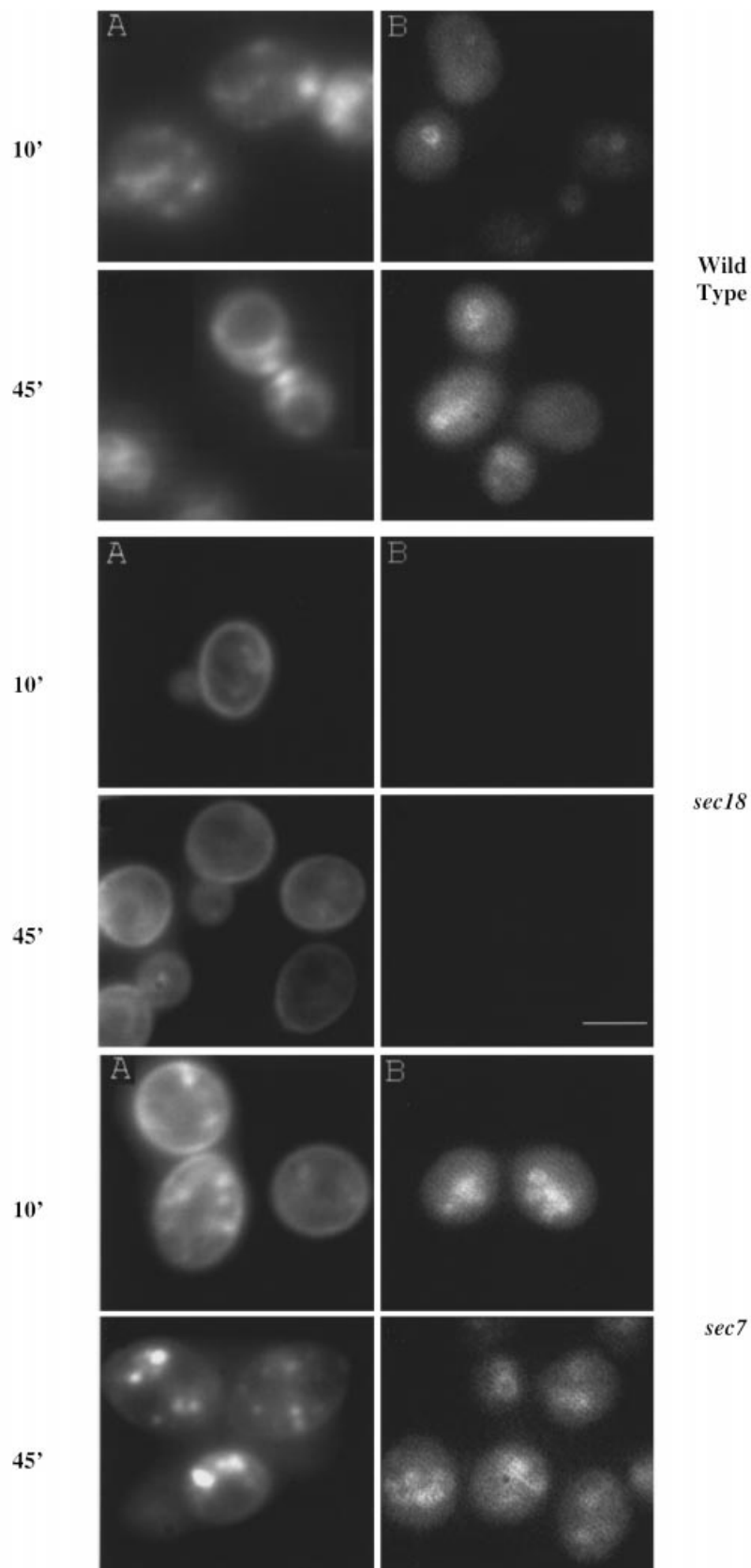


**Figure 3** Endocytosis and IQ substrate processing in wild-type, *sec18* and *sec7* yeast

Wild-type BJ926 cells (upper panels A and B), the *sec18* mutant strain SF282-1D $\alpha$  (middle panels A and B) and the *sec7* strain RSY58 (lower panels A and B) were grown at 25 °C, preshifted to 37 °C for 20 min, then incubated with 16  $\mu$ M FM4-64 (panels A) or 0.6 mM IQ-gp160 (panels B) for 10 or 45 min at the restrictive temperature. The results are representative of three experiments. Scale bar = 5  $\mu$ m.

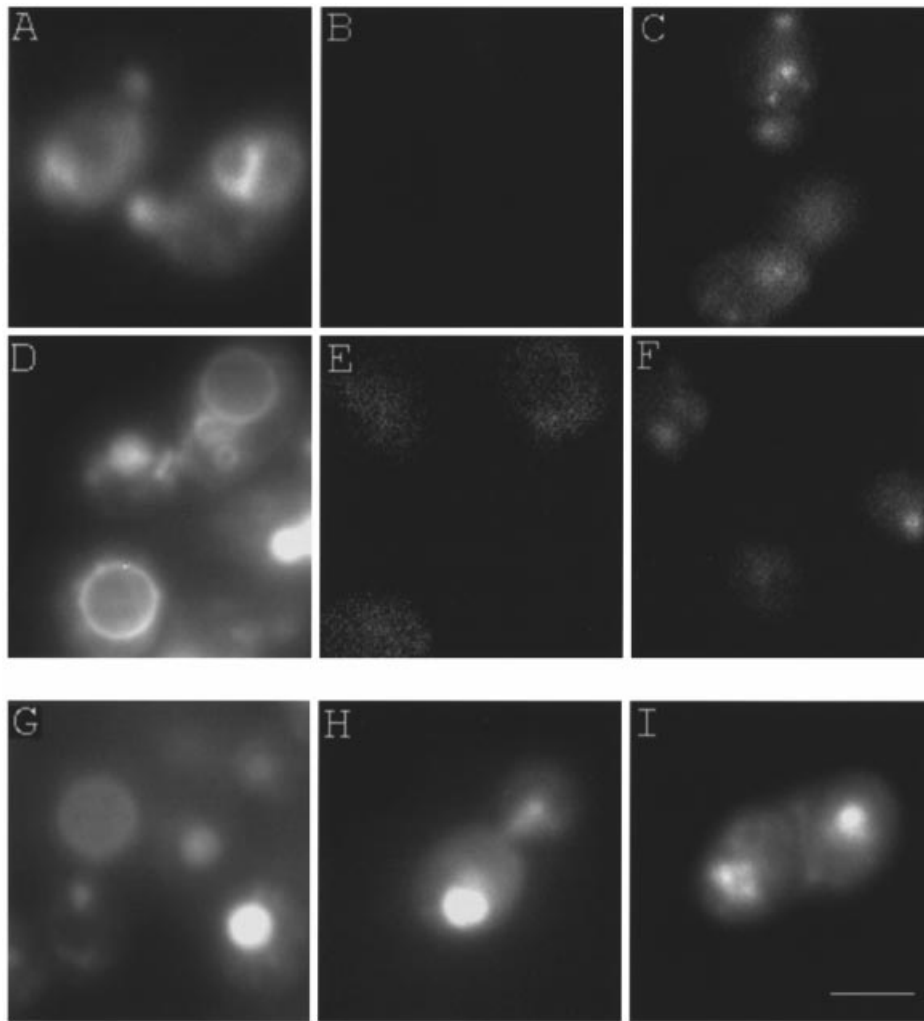


**Figure 4** Inhibition of Kex2-dependent IQ-gp160 processing in the endocytic pathway

BJ926 yeast was pretreated at 25 °C for 30 min with amidine-containing peptidyl phosphonate compounds, K-R inhibitor (A, B, D, E, H) or S-R derivative (C, F, G, I), then incubated with 16  $\mu$ M FM4-64 (A, D, G), 0.6 mM IQ-gp160 (B, C, E, F) or 0.6 mM IQ-gp160R > A (H, I) for 30 (A–C) or 60 min (D–I) before viewing by fluorescence microscopy. The results are representative of five experiments. Scale bar = 5  $\mu$ m.

IQ-gp160 processing occurred temporally sooner and in morphologically different compartments within the yeast cell than the fluorescence released by the proteolysis of the R > A peptide in the vacuole. These results indicate a cardinal requirement for a functional endocytic pathway and for active Kex2 protease to observe IQ-gp160 fluorescence in endosomes *in vivo*.

#### Inhibition of Kex2-dependent IQ substrate cleavage in yeast cells

The utility of endocytic delivery to access Kex2 protease was further investigated by incubating intact yeast with small-molecule protease inhibitors. Inhibitors that efficiently block the activity of the SPC serine protease family have previously been described [31,37,38]. The most potent inhibitor, a peptidyl (Pro-NorVal-Tyr-Lys-Arg) chloromethane, exhibits a  $K_i$  of 3.7 nM for Kex2, *in vitro* [37]. However, the alkylating chloromethane derivatives were very toxic to cells, independent of their specific inhibition of SPC proteases [38]. Since protease inhibitors were to be used in this study with intact cells, we tested the effects of amidine-containing peptidyl phosphonates on Kex2 activity *in*

*vitro*. Amidine-containing peptidyl phosphonate derivatives bind irreversibly to the catalytic domains of blood coagulation and related serine proteases [26]. We tested two different compounds, Lys-Arg phosphonate (K-R inhibitor) and a Ser-Arg derivative (S-R derivative), on ssKex2 cleavage of the fluorogenic IQ-gp160 substrate. After a 15 min preincubation with ssKex2, the K-R inhibitor blocked Kex2 activity by ~90% at concentrations from 0.1–1 mM, whereas the S-R derivative had no effect on Kex2 protease activity (results not shown). However, both compounds inhibited trypsin cleavage activity. Furthermore, incubation of either inhibitor with live yeast cells had no apparent effect on cell viability or growth rate. Therefore, the di-residue K-R inhibitor, though lacking the potency of the tetra-residue chloromethane derivatives, blocked Kex2 activity *in vitro*, yet was not cytotoxic to yeast.

The impact of the peptidyl phosphonate derivatives on IQ substrate cleavage in intact cells was tested. Cells were exposed to the peptidyl phosphonate derivatives for 30 min, then washed and incubated with either FM4-64 dye, IQ-gp160 or IQ-gp160R > A peptides. Pretreatment with either peptidyl phosphonate

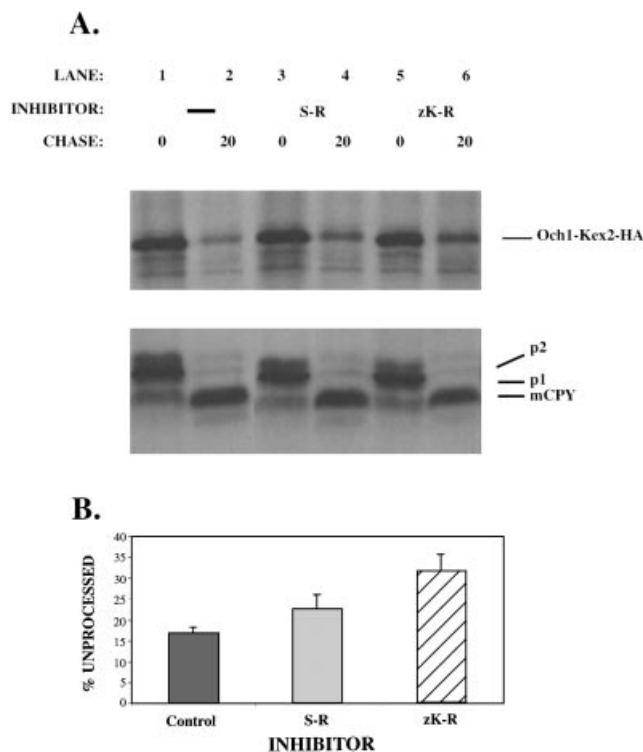


**Figure 5** Inhibition of Kex2-dependent OKH processing in the secretory pathway

(A) Top panel shows pulse–chase radiolabelling and immunoprecipitation of OKH from lysates of yeast preincubated with no inhibitor (lanes 1 and 2), 0.5 mM S-R derivative (lanes 3 and 4) or 0.5 mM K-R inhibitor (lanes 5 and 6) for 90 min, then radiolabelled with [<sup>35</sup>S]TransLabel for 10 min (0 min chase) and chased for 20 min. Och1–Kex2-HA refers to the mobility of the immunoprecipitated OKH fusion protein on SDS gel. The bottom panel shows the effects of the same conditions on CPY processing. See text for details of CPY maturation of p1 and p2 precursors to mature CPY (mCPY). (B) Quantification of OKH cleavage by PhosphorImager analysis from three experiments, as in (A). The percentage of unprocessed OKH reflects the mean ± S.E.M. ( $n = 3$ ) of the amount of immunoprecipitated OKH species remaining at 20 min chase compared with the total signal at 0 min chase.

derivative had no effect on the endocytic uptake of FM4-64 dye (Figures 4A, 4D and 4G). The S-R derivative had no effect on the appearance of fluorescence from IQ-gp160 peptide cleavage (Figure 4C). However, pretreatment of the yeast with the K-R inhibitor completely blocked the intracellular fluorescent signal resulting from IQ-gp160 processing (Figures 4B and 4E). In contrast, neither peptidyl phosphonate affected the fluorescence from IQ-gp160R > A cleavage in the vacuole (Figures 4H and 4I), suggesting that the K-R inhibitor was not broadly disruptive to proteases in the endocytic pathway.

#### Endocytic delivery of inhibitors attenuated Kex2 activity in the secretory pathway

The results from the incubation of intact yeast with substrates and inhibitors suggested that Kex2 exhibited catalytic activity in endocytic compartments, yet cellular requirements for Kex2 activity are normally attributed to the Golgi-associated processing of protein precursors in the secretory pathway. The impact of the endocytically delivered Kex2 protease inhibitors on precursor protein processing was therefore examined. The maturation of two proteins, CPY and Och1p (a type II transmembrane mannosyltransferase), was monitored by pulse–chase radio-

labelling and immunoprecipitation experiments. CPY is synthesized as an inactive precursor that is N-glycosylated *en route* to the vacuole with proteolytic processing of the inactive CPY precursor for maturation to the active species. The core-glycosylated 67 kDa endoplasmic reticulum form (p1) receives outer-chain mannoses in the Golgi to become the fully glycosylated 69 kDa (p2) species. The mature 61 kDa polypeptide is generated by proteinase A-dependent processing in the vacuole [39]. In this pulse–chase labelling regimen, the biosynthesis and maturation of CPY in the vacuole is complete by 20 min chase (Figure 5A, lower panel, lanes 1 and 2).

The other protein examined in these experiments was Och1p. This membrane protein is localized during steady state in the early Golgi, yet its normal itinerary includes access to the Kex2-containing late Golgi compartments, followed by retrieval back to the early Golgi [24,40]. To monitor its trafficking itinerary, a Kex2 consensus cleavage site followed by a HA epitope tag was fused to the luminal domain at the C-terminus of Och1p, creating an OCH1–Kex2-HA (OKH) construct. Harris and Waters [24] demonstrated by pulse–chase labelling that the HA tag was processed from the OKH construct within 5–20 min in a Kex2-dependent manner [24]. For the experiments in this study, Kex2 cleavage efficiency was quantified by the fraction of pulse–chase radiolabelled OKH polypeptide that could be precipitated with antibodies to the HA epitope. We observed that 85% of the HA epitope was processed from the OKH precursor during the 20 min chase period under normal conditions (Figure 5, top panel, lanes 1 and 2).

The influence of the peptidyl phosphonates on OKH and CPY processing was examined. Yeast cells were treated for 90 min at 25 °C with medium containing 0.5 mM peptidyl phosphonates before pulse–chase radiolabelling. Pretreatment of the cells with the K-R inhibitor reduced OKH processing to 67% (Figure 5A, top panel, lanes 5 and 6, with quantification shown in Figure 5B). However, pre-incubation with the S-R derivative showed very little reduction of OKH processing compared with the control (Figure 5A, lanes 3 and 4). Furthermore, none of the peptidyl phosphonate derivatives had any effect on CPY maturation (Figure 5A, lower panel), demonstrating that the decrease in OKH processing was not due to a broad inhibition of proteolytic processing or a general reduction in secretory pathway function. Therefore, these results suggested that the endocytic delivery of protease inhibitors interfered with Kex2 activity towards precursor protein trafficking in the secretory pathway.

#### DISCUSSION

In this report we demonstrate that endocytosis into intact cells can be utilized to deliver small molecules that interact with catalytically active Kex2 protease, which cycles through endosomes during its trafficking itinerary [17]. IQ fluorogenic peptides with paired basic amino acids are cleaved *in vitro* and *in vivo* in a sequence-specific manner by the Kex2 protease. The fluorogenic events with IQ peptides correlate with the time-course established by monitoring the uptake of FM4-64 membrane dye through endosomes to the vacuole (Figure 2 and [29]). The IQ-gp160R > A peptide, which harbours a single amino acid change at the Kex2 recognition site, is cleaved by hydrolases in the yeast vacuole. Cleavage of the IQ-gp160R > A peptide in the vacuole supports that these small peptides are transiting the endocytic pathway with fidelity, rather than being aberrantly sorted to the Golgi compartments. The Kex2-dependent cleavage of IQ-gp160 is therefore postulated to occur in endosomes. Blocking peptide and FM4-64 internalization in *sec18* mutants at the restrictive

temperature prevented substrate access and the appearance of fluorescence in the endosomes. The accumulation of fluorescent signal in these intracellular compartments in *sec7* mutants that block endocytic traffic from endosomes *en route* to the vacuole (Figure 3 and [36]) supports the hypothesis that Kex2 cleaves the IQ-gp160 peptide in endosomes. Furthermore, the endocytic delivery of peptidyl phosphonate inhibitors causes disruption of Kex2-dependent IQ-gp160 cleavage in endosomes *in vivo*, but not IQ-gp160R>A processing by hydrolases in the vacuole. Taken together, proper functioning of the endocytic pathway is essential to access catalytically active Kex2 protease in endosomes.

### Endocytic delivery affects protein processing in the secretory pathway

The modulation of precursor protein processing by the endocytic administration of soluble protease inhibitors can potentially be used to control virus infectivity. The maturation of glycoproteins of numerous enveloped viruses is dependent on the activity of the SPC proteases. The processing of these glycoprotein precursors is essential to their membrane fusion function in viral infectivity [41]. One example is the HIV-1 envelope protein gp160, which is cleaved into its functional subunits gp120 and gp41 by an SPC protease [23,38,42–44]. The concept of modulating SPC protease function by endocytic delivery was demonstrated by blocking the cleavage of the Semliki Forest virus p62 glycoprotein precursor by the endocytosis of anti-SPC protease antibodies [45].

In this study, we found that processing of the Och1p fusion protein in the secretory pathway was significantly, but not completely, disrupted by the endocytic delivery of Kex2 inhibitors (Figure 5). Several possibilities would explain the incomplete Kex2 inhibition by the endocytic delivery of peptidyl phosphonates. First, it has been estimated that  $\sim 45$  nl of fluid is internalized each hour by  $1.4 \times 10^8$  yeast cells, meaning that one cell-surface-equivalent of yeast plasma membrane is internalized in 4 h [15,46]. Secondly, the  $IC_{90}$  of inhibition by the K-R phosphonate *in vitro* reflects poor affinity of binding to the Kex2 protease. As these inhibitors act competitively with natural substrates, the accumulation of sub-mM concentrations of inhibitor would have to be achieved in endosomes for productive inhibition *in vivo*. Thirdly, the Kex2 synthesized during the course of the pretreatment represents a naive protease population that had not been exposed to endocytically delivered inhibitor. Therefore, based on the observed rate of Kex2 cycling, pre-incubation of yeast with the peptidyl phosphonate inhibitors for 1 h would access  $\sim 50\%$  of the Kex2 population [47–49]. The uninhibited Kex2 pool is therefore still available for processing substrates in the secretory pathway. Taken together, it is not surprising that Kex2 activity is not completely abolished by incubation of the K-R inhibitor with intact yeast. However, the accessibility of SPC proteases by endocytic delivery, combined with the development of more efficacious inhibitors, holds promise for treating viral infections and physiological processes dependent on precursor protein processing in the secretory pathway.

We thank Dr. Bill Betz and Dr. Steve Fadul for the use of their microscope and computer imaging software, and Dr. Rock Levinson for the use of his spectrofluorimeter. We gratefully acknowledge Dr. Sandi Harris, Dr. Gerry Waters, Dr. Vytas Bankaitis and Dr. Bob Fuller for providing strains and plasmids. Stimulating discussions with Dr. Bob Fuller, Dr. Alexander Sorkin, Dr. Kathryn Howell and members of the A.F. laboratory have contributed greatly to this work. This research was supported by National Institutes of Health grant AI-34747 to A.F., and grants from Fundação de Amparo a Pesquisa do Estado de Sao Paulo, Brazil to L.J.

### REFERENCES

- Seidah, N. G., Chretien, M. and Day, R. (1994) *Biochimie* **76**, 197–209
- Steiner, D. F., Smeekens, S. P., Ohagi, S. and Chan, S. J. (1992) *J. Biol. Chem.* **267**, 23435–23438
- Nakayama, K. (1997) *Biochem. J.* **327**, 625–635
- Julius, D., Schekman, R. and Thorner, J. (1984) *Cell* **36**, 309–318
- Julius, D., Brake, B. L., Kunisawa, R. and Thorner, J. (1984) *Cell* **37**, 1075–1089
- Franzusoff, A., Redding, K., Crosby, J., Fuller, R. S. and Schekman, R. (1991) *J. Cell Biol.* **112**, 27–37
- Redding, K., Holcomb, C. and Fuller, R. S. (1991) *J. Cell Biol.* **113**, 527–538
- Whitters, E. A., McGee, T. P. and Bankaitis, V. A. (1994) *J. Biol. Chem.* **269**, 28106–28117
- Cunningham, K. W. and Wickner, W. T. (1989) *Yeast* **4**, 17–26
- Bryant, N. and Boyd, A. (1993) *J. Cell Sci.* **106**, 815–822
- Franzusoff, A. and Schekman, R. (1989) *EMBO J.* **8**, 2695–2702
- Franzusoff, A. (1992) *Seminars Cell Biol.* **3**, 309–324
- Nothwehr, S. F. and Stevens, T. H. (1994) *J. Biol. Chem.* **269**, 10185–10188
- Seeger, M. and Payne, G. S. (1992) *J. Cell Biol.* **118**, 531–540
- Wilsbach, K. and Payne, G. S. (1993) *Trends Cell Biol.* **3**, 426–431
- Graham, T. R. and Emr, S. D. (1991) *J. Cell Biol.* **114**, 207–218
- Conibear, E. and Stevens, T. H. (1998) *Biochim. Biophys. Acta* **1404**, 211–230
- Piper, R. C., Cooper, A. A., Yang, H. and Stevens, T. H. (1995) *J. Cell Biol.* **131**, 603–617
- Wendland, B., Emr, S. D. and Riezman, H. (1998) *Curr. Opin. Cell Biol.* **10**, 513–522
- Preuss, D., Mulholland, J., Franzusoff, A., Segev, N. and Botstein, D. (1992) *Mol. Biol. Cell* **3**, 789–803
- Prescianotto-Baschong, C. and Riezman, H. (1998) *Mol. Biol. Cell* **9**, 173–189
- Brenner, C. and Fuller, R. S. (1992) *Proc. Natl. Acad. Sci. U.S.A.* **89**, 922–926
- Franzusoff, A., Volpe, A., Josse, D., Pichuantes, S. and Wolf, J. R. (1995) *J. Biol. Chem.* **270**, 3154–3159
- Harris, S. L. and Waters, M. G. (1996) *J. Cell Biol.* **132**, 985–998
- Hirata, I. Y., Cezari, M. H. S., Nakaie, C. R., Boschkov, P., Ito, A. S., Juliano, M. A. and Juliano, L. (1994) *Lett. Pept. Sci.* **1**, 299–308
- Oleksyszyn, J., Boduszek, B., Kam, C.-M. and Powers, J. C. (1994) *J. Med. Chem.* **37**, 226–231
- Henkel, A. W. and Bieger, S. C. (1994) *Anal. Biochem.* **223**, 329–331
- Chagas, J. R., Juliano, L. and Prado, E. S. (1991) *Anal. Biochem.* **192**, 419–425
- Vida, T. A. and Emr, S. D. (1995) *J. Cell Biol.* **128**, 779–792
- Betz, W. J., Mao, F. and Bewick, G. S. (1992) *J. Neurosci.* **12**, 363–375
- Jean, F., Basak, A., DiMaio, J., Seidah, N. G. and Lazure, C. (1995) *Biochem. J.* **307**, 689–695
- Angliker, H., Neumann, U., Molloy, S. S. and Thomas, G. (1995) *Anal. Biochem.* **224**, 409–412
- Rockwell, N. C., Wang, G. T., Krafft, G. A. and Fuller, R. S. (1997) *Biochemistry* **36**, 1912–1917
- Johanning, K., Juliano, M. A., Juliano, L., Lazure, C., Lamango, N. S., Steiner, D. F. and Lindberg, I. (1998) *J. Biol. Chem.* **273**, 22672–22680
- Rockwell, N. C. and Fuller, R. S. (1998) *Biochemistry* **37**, 3386–3391
- Hicke, L., Zanolari, B., Pypaert, M., Rohrer, J. and Riezman, H. (1997) *Mol. Biol. Cell* **8**, 13–31
- Angliker, H., Wikstrom, P., Shaw, E., Brenner, C. and Fuller, R. S. (1993) *Biochem. J.* **293**, 75–81
- Hallenberger, S., Bosch, V., Angliker, H., Shaw, E., Klenk, H.-D. and Garten, W. (1992) *Nature (London)* **360**, 358–361
- Stevens, T., Esmon, B. and Schekman, R. (1982) *Cell* **30**, 439–448
- Nakayama, K., Nagasu, T., Shimma, Y., Kuromitsu, J. and Jigami, Y. (1992) *EMBO J.* **11**, 2511–2519
- McCune, J. M., Rabin, L. B., Feinberg, M. B., Lieberman, M., Kosek, J. C., Reyes, G. R. and Weissman, I. L. (1988) *Cell* **53**, 55–67
- Miranda, L., Wolf, J. R., Pichuantes, S., Duke, R. and Franzusoff, A. (1996) *Proc. Natl. Acad. Sci. U.S.A.* **93**, 7695–7700
- Vollenweider, F., Benjannet, S., Decroly, E., Savaria, D., Lazure, C., Thomas, G., Chretien, M. and Seidah, N. G. (1996) *Biochem. J.* **314**, 521–532
- Decroly, E., Wouters, S., Di Bello, C., Lazure, C., Ruysschaert, J.-M. and Seidah, N. G. (1996) *J. Biol. Chem.* **271**, 30442–30450
- Sariola, M., Saraste, J. and Kuismanen, E. (1995) *J. Cell Sci.* **108**, 2465–2475
- Riezman, H. (1993) *Trends Cell Biol.* **3**, 273–277
- Wilcox, C. A., Redding, K., Wright, R. and Fuller, R. S. (1992) *Mol. Biol. Cell* **3**, 1353–1371
- Cereghino, J. L., Marcusson, E. G. and Emr, S. D. (1995) *Mol. Biol. Cell* **6**, 1089–1102
- Redding, K., Seeger, M., Payne, G. S. and Fuller, R. S. (1996) *Mol. Biol. Cell* **7**, 1667–1677